

The authors would like to thank both reviewers for the constructive comments. Our replies to the comments are given below, with the original comments in black, and our response in blue. We have revised the manuscript accordingly. All changes made to the manuscript have been marked with Track-Change tool in one of submitted files.

### **Anonymous Referee #1**

This paper describes winter time NPF in the northeastern United states using the modeling predictions combined with ambient measurements of aerosol size distributions made at two sites and their contribution to CCN production. NPF is usually considered as a main source of CCN. And observations have shown that NPF usually takes place less frequently during the winter, in many locations over the world. So the results presented in this paper are interesting considering these factors. This is a well-written paper, easy to read.

We appreciate the referee's positive comments about this work.

Perhaps, the model used too high sulfuric acid concentrations to predict NPF winter?

We made long-term measurements of NPF and sulfuric acid in Ohio and our measurements show that winter time sulfuric acid does not exceed 3e6 per cubic centimeter (Erupe et al., 2010; Yu et al., 2014). And this paper claims that in order to have NPF, sulfuric acid higher than 3e6 per cubic centimeter is needed.

Related to this, at the same site in Ohio, we also found lower frequency of NPF during the winter than other seasons, very likely due to low sulfuric acid concentrations (Erupe et al., 2010; Kanawade et al., 2012).

This is a very good point. We agree that sulfuric acid concentrations ( $[H_2SO_4]$ ) are critical for NPF. The model calculates  $[H_2SO_4]$  through the balance between the photochemical production ( $SO_2+OH$ ) and condensation. The model appears to generally capture the observed values and variations of  $SO_2$  and solar radiations for the PSP site (Fig. 2b and Fig. 2c), both are important for the photochemical production of  $H_2SO_4$ . Based on the model prediction,  $[H_2SO_4]$  can reach  $\sim 1E7/cm^3$  or higher and it is during these days that nucleation is significant (Figs. 2d and 2e). As emphasized in the paper, these nucleation events are necessary to explain the observed increase in CN10 (Fig. 2e).

It is true that the model predicted  $[H_2SO_4]$  is higher than those observed (with CIMS) in Kent, Ohio during the winter (Erupe et al., 2010; Yu et al., 2014). The possible reasons for the difference remain to be investigated. One possible explanation is the well-recognized 1-2 orders-of-magnitude lower concentrations of sulfuric acid monomer measured with CIMS than the total-sulfate values measured with MARGA and the theoretical values calculated from the vapor pressure of sulfuric acid (Neitola et al., 2015).

We have added a discussion on this in the revised text:

“It should be noted that the model predicted  $[H_2SO_4]$  is higher than those observed with a chemical ionization mass spectrometer (CIMS) during the winter in Kent, Ohio (Erupe et al., 2010; Yu et al., 2014), also located in the NEUS where wintertime nucleation was observed to occur on  $\sim 17\%$  of days (Kanawade et al., 2012). The possible reasons for the difference of model-predicted and CIMS-observed  $[H_2SO_4]$  remain to be investigated. One possible explanation is that sulfuric acid molecules are bonded with base molecules (e.g. ammonia and

amines), leading to the well-recognized 1–2 orders-of-magnitude lower concentrations of sulfuric acid monomers measured with CIMS than the total-sulfate values measured with MARGA and the theoretical values calculated from the vapor pressure of sulfuric acid (Neitola et al., 2015).”

Does the model consider temperature effects on nucleation and growth? NPF becomes more favorable at lower temperatures, as shown from laboratory studies (Duplissy et al., ; Yu et al., 2017; Tiszenkel et al., 2019). If the model includes this feature, then maybe this is due to lower temperatures?

Yes. Temperature is one of the most important parameters controlling NPF. Nucleation is favored at lower temperatures but other factors ( $[H_2SO_4]$ ,  $[NH_3]$ , ionization rates, etc.) are also important. We have added a sentence emphasizing this point.

It would be nice to give some explanation why ternary ion nucleation (as opposed to neutral ternary nucleation) is important? What are the potential sources of ions in winter in the boundary layer?

The main reason is that charged clusters have a lower nucleation barrier and thus ternary ion nucleation is favored as opposed to neutral ternary nucleation. The details can be found in the reference (Yu et al., 2018) cited in the paper. The main sources of ions in winter in the boundary layer include galactic cosmic rays and radioactive materials from soils. We have added two sentences in the first paragraph of the Results session.

And is it possible to explain the growth rate from 3 nm to the CCN size with the sulfuric acid and ammonia? If not, what makes new particles grow so fast to become CCN?

As pointed out in the text (line 226 in the changes tracked version), equilibrium uptake of  $HNO_3$  also contributes to particle growth in the winter.

## **Anonymous Referee #2**

This manuscript investigates the contribution of nucleation to particle number and CCN in the eastern US using WRF-Chem-APM. The simulations show the majority of the BL number and around half of CCN0.4% from nucleation. The simulated CN10 and some gases were evaluated against measurements at 2 sites. I'm in favor of publication once some issues have been addressed.

Abstract and other places: There are statements about how the nucleation is entirely inorganic because of low biogenic emissions in winter. However, while this is a sound hypothesis, it was not explicitly tested. Please weaken the language to make it clear that the lack of organic nucleation was assumed, not a finding.

Abstract and throughout (e.g. L60-61): Please add more statements of “The model shows. . .” or “We predict. . .” etc. The current writing style likely has these statements implied, but there is a risk of this sentiment being missed by some readers, and they may think this was more than a model finding..

We would like to clarify that the lack of organic nucleation was based on model simulations, not assumptions. The model calculates biogenic emissions based on MEGAN (see Section 2.1). Yes, we have revised the relevant sentences as suggested to weaken the language.

L25-27: This sentence is strange. What is the changing paradigm of wintertime precip? This isn't discussed in the paper other than maybe one sentence at the end of the intro (L61-65, though it doesn't refer to a changing paradigm).

This is a valid point. We have deleted this sentence from the abstract.

L54-56: The statement seems incomplete. I believe the conclusion of Yu et al. (2015) was that the ion-mediated scheme they used did not have a temperature dependence, which caused it to overpredict in the summer. Yu et al. (2017) estimates a correction for the temperature dependence that may prevent the overprediction in the summer. The current statement should explain the findings better.

Not that Fangqun won't know the reference, but for completeness: Yu, F., Luo, G., Nadykto, A. B., and Herb, J.: Impact of temperature dependence on the possible contribution of organics to new particle formation in the atmosphere, *Atmos. Chem. Phys.*, 17, 4997-5005, <https://doi.org/10.5194/acp-17-4997-2017>, 2017

Yes, we have revised the statements to include the results of the 2017 paper.

L132-134: Please add the specific instruments from which data was used here.

Added as suggested.

Figure 2d: It would be useful to show the NH<sub>3</sub> values from the model averaged over the times of the AMoN site.

Added as suggested.

L177: [NH<sub>3</sub>] \*partitioning\* is calculated with ISOROPIA II

Modified as suggested.

L215: The abstract said >85% for the surface

The value given here is for the two specific sites (PSP and APP) while >85% given in the abstract is for the whole NEUS region.

Figure 3: It's confusing that there is a line for CN<sub>10</sub> due to primary particles and CCN<sub>0.4</sub> due to secondary particles. Please make them either both primary or both secondary for consistency.

We have changed CCN<sub>0.4</sub> due to SP to CCN<sub>0.4</sub> due to PP.

L240: "Apparently" doesn't seem like the right word here. It makes this seem like the CCN-CDNC connection was not expected.

This word has been deleted from the sentence.

L242: Why does it highlight the need for \*better\* representation. Has this paper found deficiencies in representation? I don't think this paper has evaluated this.

We have changed "better" to "proper".

# 1 Wintertime New Particle Formation and Its Contribution to Cloud Condensation 2 Nuclei in the Northeastern United States

3 Fangqun Yu<sup>1</sup>, Gan Luo<sup>1</sup>, Arshad Nair<sup>1</sup>, James J. Schwab<sup>1</sup>, James P. Sherman<sup>2</sup>, and Yanda Zhang<sup>1</sup>

4 <sup>1</sup>Atmospheric Sciences Research Center, State University of New York, Albany, New York 12203, USA

5 <sup>2</sup>Department of Physics and Astronomy, Appalachian State University, NC 28608, USA

6 **Abstract:** Atmospheric particles can act as cloud condensation nuclei (CCN) and modify cloud  
7 properties and precipitation and thus indirectly impact the hydrological cycle and climate. New  
8 particle formation (NPF or nucleation), frequently observed at locations around the globe, is an  
9 important source of ultrafine particles and CCN in the atmosphere. In this study, wintertime NPF  
10 over the Northeastern United States (NEUS) is simulated with WRF-Chem coupled with a size-  
11 resolved (sectional) advanced particle microphysics (APM) model. Model simulated variations of  
12 particle number concentrations during a two-month period (November–December 2013) are in  
13 agreement with corresponding measurements taken at Pinnacle State Park (PSP), New York and  
14 Appalachian State University (APP), North Carolina. We show that even during wintertime,  
15 regional nucleation occurs and contributes significantly to ultrafine particle and CCN number  
16 concentrations over the NEUS. ~~The model shows that, d~~Due to low biogenic emissions during this  
17 period, wintertime regional nucleation is solely controlled by inorganic species and the newly  
18 developed ternary ion-mediated nucleation scheme is able to capture the variations of observed  
19 particle number concentrations (ranging from  $\sim 200 - 20,000 \text{ cm}^{-3}$ ) at both PSP and APP. Total  
20 particle and CCN number concentrations dramatically increase following NPF events and have  
21 highest values over the Ohio Valley region, where elevated  $[\text{SO}_2]$  is sustained by power plants.  
22 Secondary particles dominate particle number abundance over the NEUS and their fraction  
23 increases with altitude from  $>\sim 85\%$  near surface to  $>\sim 95\%$  in the upper troposphere. The  
24 secondary fraction of CCN also increases with altitude, from 20–50% in the lower boundary layer  
25 to 50–60% in the middle troposphere to 70–85% in the upper troposphere. ~~This significant  
26 contribution of wintertime nucleation to aerosols, especially those that can act as CCN, is  
27 important considering the changing paradigm of wintertime precipitation over the NEUS.~~

28

## 29 1. Introduction

30 Particle number concentration is a key parameter important for the health and climate impacts  
31 of atmospheric aerosols. High number concentrations of ultrafine particles may lead to adverse  
32 health effects (Knibbs et al., 2011; Han et al., 2016). Variations in the number concentration of  
33 cloud condensation nuclei (CCN) influence cloud properties and precipitation and thus indirectly  
34 affect the hydrological cycle and climate (e. g, Twomey, 1977; Charlson et al., 1992). Aerosol  
35 particles appear in the troposphere due to either in-situ new particle formation (NPF, i.e, formation  
36 of secondary particles (SP) via nucleation) or direct emissions (i.e., primary particles (PP)).  
37 Though NPF has little effect on the total particle mass in the immediate vicinity of the nucleation  
38 itself, it is highly relevant to the aerosol health and climate effects as SP can dominate the ultrafine  
39 particles and those particles that can act as CCN (Spracklen et al., 2008; Pierce and Adams, 2009;  
40 Yu and Luo, 2009). Aerosol number concentrations exhibit significant spatial and temporal  
41 variability due to non-linear dependence of NPF rates on atmospheric conditions and  
42 concentrations of gaseous precursors, both of which are subject to changes as a result of climate  
43 changes and emission regulatory actions.

44 Laboratory experiments and theoretical studies indicate that sulfuric acid, ammonia, amines,  
45 ions, and certain organic compounds can all contribute to NPF (see recent review paper by Lee et  
46 al., 2019). However, the actual contribution of various nucleation pathways and key controlling  
47 parameters in the real atmosphere remains elusive, especially with regard to the relative  
48 importance of inorganic versus organic nucleation (e.g., Yu et al., 2015). Inorganic and organic  
49 nucleation precursors have quite different sources and their emission strengths depend on different  
50 factors, with important implications to spatial distributions of NPF and CCN and their short-term  
51 (diurnal, seasonal) and long-term (pre-industry, present, and future climate and emissions)  
52 variations. Both inorganic and organic nucleation schemes are subject to uncertainties and it is  
53 important to evaluate their ability to capture particle formation and variations of number  
54 concentration in the atmosphere. Yu et al. (2015) showed that both inorganic nucleation and  
55 organic mediated nucleation can explain NPF observed in a spring month at several forest sites in  
56 North America but organic-mediated nucleation over-predicted NPF in the summer. [This](#)  
57 [summertime over-prediction of the organic-mediated nucleation is reduced when a temperature-](#)  
58 [dependence correction is applied \(Yu et al., 2017\).](#)

59 The main objective of the present study is to investigate the new particle formation process  
60 and its contribution to particle number concentration and CCN in the wintertime in the  
61 Northeastern United States (NEUS). Wintertime biogenic emissions are likely very low in the  
62 NEUS and thus the contribution of biogenic organic species to NPF is expected to be negligible,  
63 enabling us to unequivocally evaluate the performance of the inorganic nucleation scheme. In  
64 addition to delineating the underlying processes controlling particle number concentrations in the  
65 atmosphere, an improved understanding of major sources and concentrations of CCN in  
66 wintertime is also important for better forecasting wintertime precipitation, such as snow storms,  
67 in the NEUS (Gaudet et al., 2019).

68

## 69 **2. Methods**

### 70 2.1 Model

71 We employ WRF-Chem (version 3.7.1), a regional multi-scale meteorology model coupled  
72 with online chemistry (Grell et al., 2005). The model configurations include Morrison 2-mom  
73 microphysics (Morrison et al., 2009), RRTMG longwave and shortwave radiation (Clough et al.,  
74 2005), Noah land surface, Grell-3 cumulus (Grell and Freitas, 2014), and YSU PBL scheme (Hong  
75 et al., 2006). We use CB05 scheme (Yarwood et al., 2005) for gas-phase chemistry, SORGAM  
76 with aqueous reactions (Schell et al., 2001) for secondary organic aerosol chemistry and aqueous  
77 phase chemistry, and ISORROPIA II (Fountoukis and Nenes, 2007) for aerosol thermodynamic  
78 equilibrium. The initial and boundary conditions for meteorology are generated from the National  
79 Centers for Environmental Prediction (NCEP) Final (FNL) with resolution at  $1^{\circ} \times 1^{\circ}$  and time  
80 intervals at six hours. The anthropogenic emissions are based on the Environmental Protection  
81 Agency's (EPA) National Emission Inventory (NEI) 2011, and the biogenic emissions are  
82 calculated using the model of emissions of gases and aerosols from nature (MEGAN; \_(Guenther  
83 et al., 2006). Annual scaling factors for NO<sub>x</sub>, SO<sub>2</sub>, NH<sub>3</sub>, and CO derived from EPA's Air Pollutant  
84 Emissions Trends Data from 1990 to 2016 are used here to scale the emissions of corresponding  
85 species from the baseline year of 2011 to the simulation year. We also considered seasonal variation  
86 of NH<sub>3</sub> emission due to agricultural activity in the model.

87 For particle microphysics, we use a size-resolved (sectional) advanced particle microphysics  
88 (APM) model (Yu and Luo, 2009) that was previously integrated into WRF-Chem v3.1.1 (Luo and

89 Yu, 2011). For this study, we have updated APM and integrated it into WRF-Chem v3.7.1. Major  
90 changes to APM include: (1) employment of 15 bins to represent black carbon (BC) and another  
91 15 bins to represent primary organic carbon (POC) particles in the size range of 3 nm to 2  $\mu$ m  
92 (instead of two log-normal modes in the previous version); (2) consideration of the successive  
93 oxidation aging of secondary organic gases (SOG) and explicit kinetic condensation of low volatile  
94 SOG onto particles following the scheme of Yu (2011); (3) fully coupled APM aerosols with WRF-  
95 Chem radiation code and cloud microphysics, with aerosol optical properties and aerosol activation  
96 calculated from size-resolved APM aerosols using optical properties lookup tables (Yu et al., 2012)  
97 and the activation scheme of Abdul-Razzak and Ghan (2002). Cloud droplet number predicted by  
98 APM directly impacts spectral shape parameter and slope parameter for cloud droplets in the  
99 Morrison 2-mom microphysics scheme and then impacts cloud droplet effective radius, the auto-  
100 conversion of cloud water to rainwater, and ultimately affects the rainwater mass content and  
101 raindrop number concentration.

102 We have carried out WRF-Chem-APM simulations for the period of October 25 – December  
103 31, 2013 at 27 km  $\times$  27 km horizontal resolution. The domain covered the main continental United  
104 States, extending approximately from latitudes 21° N to 54° N and from longitudes 62° W to 132°  
105 W, with 180 grid nodes in the east–west direction and 126 in the north–south direction. The model  
106 has 30 vertical layers from the surface to 5 hPa, with finer resolution near the surface (6 layers  
107 within  $\sim$ 1 km above surface). The simulations were restarted on November 1, November 16,  
108 December 1, and December 16, 2013 with continuous chemistry fields from previous runs. The  
109 present analysis focuses on the NEUS during November and December of 2013. Simulated 3-D  
110 fields meteorological, chemical, and aerosol variables were output every three hours for each grid  
111 box and every 15 minutes at the measurement sites described below.

112

## 113 2.2 Measurement site description

### 114 2.2.1. Pinnacle State Park (PSP), Addison, New York (NY)

115 The PSP site is located in Addison, NY, a village in southwestern NY. Its coordinates are  
116 42.09°N and 77.21°W, and it is about 504 meters (m) above sea level (Schwab et al., 2009). The  
117 area surrounding PSP contains a variety of vegetation, including a golf course to the northwest;  
118 forestlands consisting of deciduous and coniferous trees; pastures and fields; and a 50-acre pond  
119 to the site’s south (Schwab et al., 2009). The two nearest population centers to PSP are Addison

120 and Corning. The village of Addison is about 4 km to the northwest of PSP, and it has a population  
121 of approximately 1800 people. The city of Corning is about 15 km to the northeast of PSP, and it  
122 has a population of approximately 11,000 people. Parameters measured include particle number  
123 concentration with a TSI model 3783 CPC, SO<sub>2</sub> with a Thermo model 43i, temperature, relative  
124 humidity, wind speed and direction, solar radiation, and precipitation with calibrated  
125 meteorological sensors. These data are collected as minute averages. Gaseous NH<sub>3</sub> is collected as  
126 part of the AMon network as passive two week samples from the nearby Connecticut Hill site  
127 (NADP, 2018).

128

### 129 2.2.2. Appalachian State University (APP), Boone, North Carolina (NC)

130 The APP site is located at 1076 m on a hill overlooking the campus of Appalachian State  
131 University (Boone, NC) in the heart of the Southern Appalachian Mountains (36.2° N, 81.7° W)  
132 (Sherman et al., 2015). The APP site is surrounded by forests in all directions and is not located  
133 near any major highways or major industry. The Charlotte metropolitan area (population 2.5  
134 million) is located approximately 160 km SE of APP and the Piedmont Triangle metropolitan area  
135 (population 1.6 million) is located 200–230 km ESE of APP. Aerosol optical and microphysical  
136 properties are measured as part of NOAA Earth System Research Laboratory (ESRL) (Sherman et  
137 al., 2015). Particle number concentrations measured with a TSI Model 3010 CPC are used in the  
138 present study.

139

## 140 3. Results

141 WRF-Chem-APM simulated wintertime NPF over the NEUS for the two-month period  
142 (November–December 2013) is examined. The nucleation rate is calculated with a recently  
143 developed H<sub>2</sub>SO<sub>4</sub>-H<sub>2</sub>O-NH<sub>3</sub> ternary ion-mediated nucleation (TIMN) scheme (Yu et al., 2018),  
144 which is supported by the detailed CLOUD (Cosmics Leaving OUtdoor Droplets) measurements  
145 (Kirkby et al., 2011; Kurten et al., 2016). According to the TIMN scheme, H<sub>2</sub>SO<sub>4</sub> and NH<sub>3</sub> are key  
146 nucleation precursors and other parameters such as temperature, relative humidity, ionization rate,  
147 and surface area of pre-existing particles also influence nucleation rates. In the presence of  
148 ionization, ternary ion nucleation is favored as opposed to neutral ternary nucleation because  
149 charged clusters have a lower nucleation barrier (Yu et al., 2018). The main sources of ions in  
150 winter in the boundary layer include galactic cosmic rays and radioactive materials from soils.

151 H<sub>2</sub>SO<sub>4</sub>, well recognized to be critical for NPF in the atmosphere, is the oxidation product of SO<sub>2</sub>.  
152 Figure 1 shows the modeled horizontal spatial distribution for the lower boundary layer (first three  
153 model layers, ~ 0 – 400 m above surface) over the NEUS during November–December 2013 of  
154 the concentrations of major aerosol precursors (a) SO<sub>2</sub> & (b) H<sub>2</sub>SO<sub>4</sub>, and (c) NH<sub>3</sub>, (d) nucleation  
155 rate (J), (e) number concentration of condensation nuclei > 10 nm (CN10), and (f) number  
156 concentration of CCN at supersaturation 0.4% (CCN0.4). Typical wintertime modeled  
157 concentrations of aerosol precursors in the lower boundary layer over the NEUS are [SO<sub>2</sub>] ~ 0.3 –  
158 2 ppbv, [H<sub>2</sub>SO<sub>4</sub>] ~ 0.03 – 0.2 pptv, and [NH<sub>3</sub>] ~ 0.1 – 5 ppbv. The modeled spatial distribution of  
159 the aerosol precursors is co-located with their source regions: SO<sub>2</sub> distribution is in line with the  
160 NEI and indicative of coal-fired power plants in the region, especially over the Ohio Valley. NH<sub>3</sub>  
161 hotspots are over emission regions of agricultural land-use and concentrated animal feeding  
162 operations. Calculated monthly mean nucleation rates in the lower boundary layer range typically  
163 from ~ 0.1 to ~ 2 cm<sup>3</sup>s<sup>-1</sup> over the NEUS domain and spatial distributions are strongly correlated  
164 with concentration of aerosol precursors, with negligible nucleation over the oceanic area off the  
165 east coast. The number concentrations of CN10 and CCN0.4, calculated from the simulated  
166 particle number size distributions, are ~ 2000–7000 cm<sup>-3</sup> and ~ 100–1000 cm<sup>-3</sup>, respectively. Both  
167 CN10 and CCN0.4 have highest values over the Ohio Valley region.

168 To develop further confidence in WRF-Chem-APM simulations, diurnal variations of these  
169 aerosol precursors, as well as meteorological factors are compared with available in situ  
170 measurements for this two-month period at the PSP site in Figure 2. The meteorological parameters  
171 compared are temperature (T) at 2 m above surface, relative humidity (RH), wind direction, solar  
172 radiation, and precipitation in Figure 2 (a–c). Overall, WRF-Chem-APM simulates the diurnal  
173 variations of T and RH in good agreement with measurements (Fig. 3a), with Pearson correlation  
174 coefficient (*r*) of 0.93 for hourly T and 0.74 for hourly RH. The model also captures major changes  
175 in wind direction (Fig. 2b), solar radiation (Fig. 2b), and occurrence of precipitation (Fig. 2c). The  
176 model slightly over-predicted RH and T. It should be noted that RH measurements were taken at  
177 2 m above surface while modeled RH is the average of model surface layer (~ 0–100 m). The  
178 differences/deviations during some days can also be associated with model uncertainties and sub-  
179 grid variations within the 27 km × 27 km grid box. In situ measurements of [SO<sub>2</sub>] and [NH<sub>3</sub>] from  
180 the PSP site are used to examine their simulated values. Absolute values of [SO<sub>2</sub>] and their day-  
181 to-day variations (from below 0.1 ppbv to above 1 ppbv) are overall consistent with observations

182 (Fig. 2c), with  $r$  of 0.48 and mean bias error (MBE) of  $-12\%$ . The daily variation of  $[\text{NH}_3]$  (Fig.  
183 2d) is more dramatic than that of  $[\text{SO}_2]$ , with the maximum value reaching  $\sim 10$  ppbv on Day 320  
184 and minimum value approaching zero on many days. In WRF-Chem,  $[\text{NH}_3]$  partitioning is  
185 calculated with ISORROPIA II (Fountoukis and Nenes, 2007) and assumes equilibrium between  
186 gaseous and particulate phases. In addition to emission, deposition, and transport,  $[\text{NH}_3]$  is also  
187 controlled by particle compositions and temperature. The best available  $[\text{NH}_3]$  data for the site  
188 during this period is from the Ammonia Monitoring Network (AMoN), which provides 2-week  
189 averages (blue line). The average values of modeled (~~observed~~)  $[\text{NH}_3]$  during the same 2-week  
190 periods are also shown in Fig. 2d (cyan line). The modeled values are close to AMoN  
191 measurements in November and but are much lower than the observed values in December are  
192 0.26 (0.5) and 0.04 (0.2) ppbv, respectively, indicating average model–observation consistency  
193 with lower bias of model simulations. Measurements of  $[\text{NH}_3]$  at high temporal resolution are  
194 apparently needed to more rigorously evaluate the model performance.

195 Based on MEGAN, During this wintertime period, biogenic emissions during this wintertime  
196 period are low, leading to negligible modeled isoprene and monoterpene (not shown) and [LV-  
197 SOG] (Fig. 2d, generally  $< 10^6 \text{ cm}^{-3}$ ). In contrast, the peak  $[\text{H}_2\text{SO}_4]$  can reach above  $10^7 \text{ cm}^{-3}$ . As  
198 a result of its sole production from photochemistry and its short lifetime associated with  
199 condensation on pre-existing particles,  $[\text{H}_2\text{SO}_4]$  shows strong diurnal variation.  $[\text{H}_2\text{SO}_4]$  above  $\sim$   
200  $3 \times 10^6 \text{ cm}^{-3}$  is a necessary condition for substantial nucleation (with nucleation rate  $J > 0.1 \text{ cm}^{-3} \text{ s}^{-1}$ )  
201 to occur (Fig. 2e). On Days 319 and 320 (November 15-16), peak  $[\text{H}_2\text{SO}_4]$  was above  $3 \times 10^7 \text{ cm}^{-3}$   
202 and maximum nucleation rate reached up to  $10 \text{ cm}^{-3} \text{ s}^{-1}$ . It should be noted that the model predicted  
203  $[\text{H}_2\text{SO}_4]$  is higher than those observed with a chemical ionization mass spectrometer (CIMS)  
204 during the winter in Kent, Ohio (Erupe et al., 2010; Yu et al., 2014), also located in the NEUS  
205 where wintertime nucleation was observed to occur on  $\sim 17\%$  of days (Kanawade et al., 2012). The  
206 possible reasons for the difference of model-predicted and CIMS-observed  $[\text{H}_2\text{SO}_4]$  remain to be  
207 investigated. One possible explanation is that sulfuric acid molecules are bonded with base  
208 molecules (e.g. ammonia and amines), leading to the well-recognized 1–2 orders-of-magnitude  
209 lower concentrations of sulfuric acid monomers measured with CIMS than the total-sulfate values  
210 measured with MARGA and the theoretical values calculated from the vapor pressure of sulfuric  
211 acid (Neitola et al., 2015).

212 In addition to  $[H_2SO_4]$ , which also depends on surface area of pre-existing particles (and hence  
213 RH),  $[NH_3]$  and T are other two important parameters controlling the variations of nucleation rates.  
214 Lower T is known to favor nucleation according to laboratory measurements (e.g., Tiszenkel et al.,  
215 2019) and theoretical calculation (e.g., Yu et al., 2018). It should be noted that ionization rates  
216 assumed in the model, while also important for NPF under the conditions, do not have much  
217 temporal and horizontal variations. The variations of  $J$  lead to large changes of CN10, from several  
218 hundreds to above tens of thousands per  $cm^{-3}$ , which is in good agreement with observations (Fig.  
219 2e) and analyzed in more detail in Figure 3.

220 Figure 3 presents simulated surface-level (model first layer) particle number size distributions  
221 (PNSD), ~~and~~ CN10, and CCN0.4 during the two-month period for two sites in the NEUS where  
222 CN10 in situ measurements are available: (a) PSP and (b) APP. The evolution of PNSD shows  
223 clearly the occurrence of strong nucleation and growth events on some days leading to significant  
224 increase in CN10 and CCN0.4. During the winter months, photochemistry is relatively weak and  
225 MEGAN biogenic emissions are small. Nevertheless, our model simulations show that nucleated  
226 particles of a few nanometers, through  $H_2SO_4$  condensation and equilibrium uptake of  $HNO_3$ ,  $NH_3$ ,  
227 and  $H_2O$ , are able to grow to 10–30 nm on most of nucleation event days and even to 60–100 nm  
228 particles that can act as CCN during some of these days. The model captures quite well the absolute  
229 values of CN10 ( $\sim 200 - 20000 cm^{-3}$ ) as well as their daily variability at both sites, with MBE=9%,  
230 6% and  $r = 0.70, 0.55$  for the PSP and APP site, respectively. The PNSDs and CN10 time series  
231 indicate that at both sites, CN10 is dramatically elevated (by a factor of up to  $\sim 10$ ) in the aftermath  
232 of nucleation events. CN10 associated with primary particles (CN10\_PP, mainly black carbon and  
233 primary organic carbon, with coating of secondary species) remains fairly constant ( $\sim 100 cm^{-3}$ )  
234 during nucleation events. Based on the model simulation, the mean CN10 (CN10\_PP) during the  
235 two month period are 2989 (106)  $cm^{-3}$  for the PSP site and 3180 (88)  $cm^{-3}$  for the APP site, showing  
236 that the secondary particles (CN10 - CN10\_PP) account for >95% of total CN10. The  
237 concentration of CCN0.4 ~~and the fraction associated with secondary particles ( $f_{CCN\_SP}$ )~~ in the  
238 surface layer at the two sites has ve large variations, ranging from several tens to several thousand  
239 per  $cm^{-3}$ , ~~for CCN0.4 and  $\sim 0-90\%$  for  $f_{CCN\_SP}$ . CCN0.4 and  $f_{CCN\_SP}$  are generally elevated~~  
240 substantially during nucleation event days. CCN0.4 associated with primary particles (CCN0.4\_PP)  
241 is only slightly lower than CN10\_PP, indicating most of primary particles in the region are good  
242 CCNs during the winter. Based on the model simulations, the coating of secondary species on

243 primary particles increases both the size and hygroscopicity of primary particles. On average for  
244 the two-month period, primary and secondary particles each contribute to about 50% of CCN0.4  
245 near surface at the two sites.

246 For detailed examination of the contribution of nucleation to CCN0.4 at the regional scale, a  
247 four-day period (November 15–18, 2013, marked within a black rectangle in Fig. 3) is selected so  
248 as to have all permutations of nucleation events and non-events at the two sites (PSP and APP).  
249 November 15 (Day 319) has nucleation events at both sites, November 16 has nucleation event  
250 only at PSP, November 17 has nucleation non-events at both sites, and November 18 has nucleation  
251 event only at APP. Figure 4 shows for the NEUS, containing the PSP and APP sites, the modeled  
252 horizontal spatial distribution of  $[\text{SO}_2]$ ,  $[\text{H}_2\text{SO}_4]$ , and nucleation rate ( $J$ ) averaged within the  
253 boundary layer (first 7 model layers above surface).  $[\text{SO}_2]$  is controlled by emission, transport,  
254 chemistry, and deposition. Large daily variation of  $[\text{SO}_2]$  in the NEUS and the important role of  
255  $\text{SO}_2$  emission from Ohio Valley region can be clearly seen in Fig. 4. The dependence of nucleation  
256 rate on  $[\text{H}_2\text{SO}_4]$ , which is determined by  $\text{SO}_2$  oxidation production rate and condensation sink, is  
257 clear over the NEUS. Consistent with the nucleation events and non-events observed at PSP and  
258 APP sites during the 4-day period as shown in Fig. 3, Figure 4 shows that the nucleation is  
259 generally at the regional scale with spatial distribution similar to that of  $[\text{H}_2\text{SO}_4]$ . These regional  
260 wintertime nucleation events contribute significantly to CCN0.4 in the NEUS as evidenced in the  
261 day-to-day spatial variations in CCN0.4 given in Fig. 5 (upper panels). Regions of high CCN0.4,  
262 generally dominated by secondary particles (Fig. 5 middle panes), correspond well with areas of  
263 high nucleation (Fig. 4, lower panels)). More than  $\sim 80\%$  of CCN0.4 is of secondary origin in  
264 regions with CCN0.4 above  $\sim 1000 \text{ cm}^{-3}$ . Figure 5 (lower panels) also gives daily mean Cloud  
265 Droplet Number Concentration (CDNC) in the boundary layer (liquid water content weighted  
266 average) during the period. ~~Apparently, C~~louds formed in regions of higher CCN0.4 have larger  
267 CDNC and secondary particles contribute to CDNC in these regions, highlighting the need for  
268 ~~better-proper~~ representation of secondary particle formation and growth in regional models.

269 So far, our analysis focuses on aerosol and precursors near surface or in the boundary layer. To  
270 examine the vertical variations, Figure 6 shows the two-month (November–December 2013) mean  
271 nucleation rates and consequent contribution to CN10 (SP fraction,  $f_{\text{CN10\_SP}}$ ) and CCN0.4 (SP  
272 fraction,  $f_{\text{CCN\_SP}}$ ) in the lower boundary layer (below  $\sim 960 \text{ mb}$ ), lower troposphere ( $\sim 960\text{--}800$   
273  $\text{mb}$ ), middle troposphere ( $\sim 800\text{--}470 \text{ mb}$ ), and upper troposphere ( $\sim 470\text{--}250 \text{ mb}$ ) over the NEUS.

274 The model simulations indicate substantial nucleation at all altitudes although nucleation rates are  
275 higher in lower boundary layer and upper troposphere. Horizontal distributions of nucleation rates  
276 in lower boundary layer and lower troposphere differ significantly from those in middle and upper  
277 troposphere, indicating quite different sources of air mass and that the influence of local emission  
278 is limited to the lower troposphere. Secondary particles dominate CN10 at all altitudes over the  
279 NEUS and  $f_{\text{CN10\_SP}}$  increases with altitudes from  $>\sim 85\%$  in lower boundary layer to  $>\sim 95\%$  in the  
280 upper troposphere. In the lower boundary layer, secondary particles formed via nucleation  
281 contribute to the CCN0.4 number concentration from about 20-30% over the New England region  
282 to  $\sim 40\text{--}50\%$  over the Ohio Valley region. Similar to that of CN10, the SP fraction of CCN0.4  
283 increases with altitudes, reaching to 50-60% in the middle troposphere and 70-85% in the upper  
284 troposphere

285

#### 286 4. Summary

287 New particle formation (NPF) has been well recognized as an important source of ultrafine  
288 particles which can lead to adverse health impacts and CCN which affects cloud, precipitation, and  
289 climate. In this study, wintertime particle formation over the Northeastern United States (NEUS)  
290 and its contribution to particle number concentrations and CCN are investigated. Wintertime NPF  
291 in the NEUS is expected to be dominated by inorganic species as a result of very low biogenic  
292 emissions. Based on WRF-Chem-APM simulations for a two-month period (November–  
293 December 2013) and comparisons with measurements, we show that substantial regional scale  
294 NPF occurs in the winter over the NEUS despite weaker photochemistry and low MEGAN  
295 biogenic emissions. The recently developed physics-based  $\text{H}_2\text{SO}_4\text{-H}_2\text{O-NH}_3$  ternary ion-mediated  
296 nucleation scheme appears to be able to capture the absolute values of particle number  
297 concentrations as well as their daily variations observed at two sites in NEUS. The freshly  
298 nucleated nanometer particles can grow to 10-30 nm on most nucleation event days and to CCN  
299 sizes during some of these days. CN10 and CCN0.4 are dramatically elevated in the aftermath of  
300 nucleation events. Calculated monthly mean nucleation rates in the boundary layer over the NEUS  
301 range from  $\sim 0.1$  to  $\sim 2 \text{ cm}^3\text{s}^{-1}$  and spatial distributions are strongly correlated with concentration  
302 of aerosol precursors. The monthly mean number concentrations of CN10 and CCN0.4 are around  
303  $2000\text{--}7000 \text{ cm}^{-3}$  and  $100\text{--}1000 \text{ cm}^{-3}$ , respectively. Both CN10 and CCN0.4 have highest values  
304 over the Ohio Valley region, a key source region of anthropogenic  $\text{SO}_2$ . The model simulations

305 indicate substantial nucleation occurs at all altitudes although nucleation rates are higher in lower  
306 boundary and upper troposphere. Secondary particles dominate CN10 at all altitudes over NEUS  
307 and its fraction increases with altitudes from >~85% near surface to >~95% in upper troposphere.  
308 The fraction of CCN0.4 due to secondary particles also increases with altitudes, from 20-50% in  
309 the lower boundary layer to 50-60% in the middle troposphere and 70–85% in the upper  
310 troposphere.

311

312 **Data availability.** The model output and observational data used for comparison are available on  
313 request from the authors.

314 **Author contributions.** FY, GL, and YZ developed the project idea. GL and FY updated the model  
315 and carried out the numerical simulations. FY and AN wrote the paper, with contribution from GL  
316 and JJS. JJS and JBS contributed observational data used in the comparison.

317 **Competing interests.** The authors declare that they have no conflict of interest.

318 **Acknowledgements:** This study was supported by NYSERDA under contract 100416 and NSF  
319 under grants OISE-1545917 and AGS-1550816, and Ammonia Monitoring Network (AMoN)  
320 data used for comparison is from National Atmospheric Deposition Program (NRSP-3), 2017,  
321 NADP Program Office, Illinois State Water Survey, University of Illinois, Champaign, IL 61820  
322 (<http://nadp.sws.uiuc.edu/AMoN/>).

## 323 **References**

324 Abdul-Razzak, H., and Ghan, S. J., A parameterization of aerosol activation, 3, Sectional  
325 representation, *J. Geophys. Res.*, 107( D3), doi:10.1029/2001JD000483, 2002.

326 Charlson R. J., Schwartz S. E., Hales J. M., Cess R. D., Coakley J. A., Jr., Hansen J. E. and  
327 Hofmann D. J. Climate forcing by anthropogenic aerosols. *Science* 255, 423-430, 1992.

328 Clough, S. A., M. W. Shephard, E. J. Mlawer, J. S. Delamere, M. J. Iacono, K. Cady-Pereira, S.  
329 Boukabara, and P. D. Brown, Atmospheric radiative transfer modeling: A summary of the  
330 AER codes, *J. Quant. Spectrosc. Radiat. Transfer*, 91, 233–244,  
331 doi:10.1016/j.jqsrt.2004.05.058, 2005.

332 [Erupe, M. E., D. R. Benson, J. Li., L.-H. Young, B. Verheggen, M. Al-Refai, O. Tahboub, V.](#)  
333 [Cunningham, F. Frimpong., A. A. Viggiano and S.-H. Lee, Correlation of aerosol nucleation](#)

334 [rate with sulfuric acid and ammonia in Kent Ohio: an atmospheric observation, J. Geophys.](#)  
335 [Res., 115, Doi:10.1029/2010JD013942, 2010.](#)

336 Fountoukis, C., and A. Nenes, ISORROPIA II: A computationally efficient thermodynamic  
337 equilibrium model for  $K^+$ - $Ca^{2+}$ - $Mg^{2+}$ - $NH_4^+$ - $Na^+$ - $SO_4^{2-}$ - $NO_3^-$ - $Cl^-$ - $H_2O$  aerosols, *Atmos.*  
338 *Chem. Phys.*, 7(17), 4639–4659, doi:10.5194/acp-7-4639-2007, 2007.

339 Gaudet, L. C., K. J. Sulia, F. Yu, and G. Luo, Sensitivity of Lake-Effect Cloud Microphysical  
340 Processes to Ice Crystal Habit and Nucleation during OWLeS IOP4, *J. of Climate*,  
341 <https://doi.org/10.1175/JAS-D-19-0004.1>, 2019.

342 Grell, G. A. and Freitas, S. R.: A scale and aerosol aware stochastic convective parameterization  
343 for weather and air quality modeling, *Atmos. Chem. Phys.*, 14, 5233-5250,  
344 <https://doi.org/10.5194/acp-14-5233-2014>, 2014.

345 Grell, G. A., Peckham, S. E., McKeen, S., Schmitz, R., Frost, G., Skamarock, W. C., and Eder, B.:  
346 Fully coupled “online” chemistry within the WRF model, *Atmosph. Env.*, 39, 6957–  
347 6975, 2005.

348 Guenther, A., Karl, T., Harley, P., Wiedinmyer, C., Palmer, P. I., and Geron, C.: Estimates of  
349 global terrestrial isoprene emissions using MEGAN (Model of Emissions of Gases and  
350 Aerosols from Nature), *Atmos. Chem. Phys.*, 6, 3181-3210, [https://doi.org/10.5194/acp-6-](https://doi.org/10.5194/acp-6-3181-2006)  
351 3181-2006, 2006.

352 Han, Y., T. Zhu, T. Guan, Y. Zhu, J. Liu, Y. Ji, S. Gao, F. Wang, H. Lu, W. Huang, Association  
353 between size-segregated particles in ambient air and acute respiratory inflammation, *Science*  
354 *of The Total Environment*, 565, 412-419, 2016.

355 Hong, S.-Y., Noh, Y., Dudhia, J., A new vertical diffusion package with an explicit treatment of  
356 entrainment processes. *Mon. Weather Rev.* 134 (9), 2318–2341, 2006.

357 [Kanawade, V. P., D. R. Benson, and S.-H. Lee, Statistical analysis of 4-year observations of](#)  
358 [aerosol sizes in a semi-rural continental environment, \*Atmos. Environ.\* 59, 30-38, 2012.](#)

359 Kirkby, J. and co-authors, Role of sulphuric acid, ammonia and galactic cosmic rays in  
360 atmospheric aerosol nucleation, *Nature*, 476, 429–433, 2011.

361 Knibbs, L.D., Cole-Hunter, T., Morawska, L., A review of commuter exposure to ultrafine particles  
362 and its health effects. *Atmos. Environ.* 45, 2611-2622.  
363 <http://dx.doi.org/10.1016/j.atmosenv.2011.02.065>, 2011

364 Kürten, A., Bergen, A., Heinritzi, M., Leiminger, M., Lorenz, V., Piel, F., Simon, M., Sitals, R.,

365 Wagner, A. C., and Curtius, J.: Observation of new particle formation and measurement of  
366 sulfuric acid, ammonia, amines and highly oxidized organic molecules at a rural site in central  
367 Germany, *Atmos. Chem. Phys.*, 16, 12793–12813, <https://doi.org/10.5194/acp-16-12793-2016>,  
368 2016.

369 Lee, S.-H., Gordon, H., Yu, H., Lehtipalo, K., Haley, R., Li, Y., and Zhang, R.: New particle  
370 formation in the atmosphere: From molecular clusters to global climate, *J. Geophys. Res.*, 124,  
371 <https://doi.org/10.1029/2018JD029356>, 2019.

372 Luo, G., and F. Yu, Simulation of particle formation and number concentration over the Eastern  
373 United States with the WRF-Chem + APM model, *Atmos. Chem. Phys.*, 11, 11521-11533,  
374 [doi:10.5194/acp-11-11521-2011](https://doi.org/10.5194/acp-11-11521-2011), 2011.

375 Morrison, H., G. Thompson, and V. Tatarskii, Impact of cloudmicrophysics on the development  
376 of trailing stratiform precipitation in a simulated squall line: Comparison of one- and two-  
377 moment schemes, *Mon. Weather Rev.*, 137, 991–1007, [doi:10.1175/2008MWR2556.1](https://doi.org/10.1175/2008MWR2556.1), 2009.

378 NADP, National Atmospheric Deposition Program 2017 Annual Summary. Wisconsin State  
379 Laboratory of Hygiene, University of Wisconsin-Madison, WI. Available at:  
380 <http://nadp.slh.wisc.edu/lib/dataReports.aspx>, 2018.

381 [Neitola, K., Brus, D., Makkonen, U., Sipilä, M., Mauldin III, R. L., Sarnela, N., Jokinen, T.,](#)  
382 [Lihavainen, H., and Kulmala, M.: Total sulfate vs. sulfuric acid monomer concentrations in](#)  
383 [nucleation studies, \*Atmos. Chem. Phys.\*, 15, 3429–3443, \[https://doi.org/10.5194/acp-15-3429-\]\(https://doi.org/10.5194/acp-15-3429-2015\)](#)  
384 [2015, 2015.](#)

385 Pierce, J. R. and Adams, P. J.: Uncertainty in global CCN concentrations from uncertain aerosol  
386 nucleation and primary emission rates, *Atmos. Chem. Phys.*, 9, 1339–1356, [doi:10.5194/acp-](https://doi.org/10.5194/acp-9-1339-2009)  
387 [9-1339-2009](https://doi.org/10.5194/acp-9-1339-2009), 2009.

388 Schell B., I.J. Ackermann, H. Hass, F.S. Binkowski, and A. Ebel, Modeling the formation of  
389 secondary organic aerosol within a comprehensive air quality model system, *Journal of*  
390 *Geophysical research*, 106, 28275-28293, 2001.

391 Schwab, J.J.; Spicer, J.B.; Demerjian, K.L. Ozone, Trace Gas, and Particulate Matter  
392 Measurements at a Rural Site in Southwestern New York State: 1995-2005. *J. Air Waste*  
393 *Manage. Assoc.* 59, 293 – 309, [doi: 10.3155/1047-3289.59.3.293](https://doi.org/10.3155/1047-3289.59.3.293), 2009.

394 Sherman, J.P., P.J. Sheridan, J.A. Ogren, E.A. Andrews, L. Schmeisser, A. Jefferson, and S.  
395 Sharma, A multi-year study of lower tropospheric aerosol variability and systematic

396 relationships from four North American regions, *Atmos. Chem. Phys.*, 15, 12487-12517,  
397 doi:10.5194/acp-15-12487-2015, 2015.

398 Spracklen, D., Carslaw, K., Kulmala, M., Kerminen, V.-M., Sihto, S.-L., Riipinen, I., Merikanto,  
399 J., Mann, G., Chipperfield, M., Wiedensohler, A., Birmili, W., and Lihavainen,  
400 H.: Contribution of particle formation to global cloud condensation nuclei concentrations,  
401 *Geophys. Res. Lett.*, 35, L06808, doi:10.1029/2007GL033038, 2008.

402 [Tiszenekel, L., C. Stangl, J. Krasnomowitz, Q. Ouyang, H. Yu, M. J. Apsokardu, M. V. Johnston,](#)  
403 [S.-H. Lee, Temperature effects on sulfuric acid aerosol nucleation and growth: Initial results](#)  
404 [from the TANGENT study, \*Atmos. Chem. Phys.\*, 19, 8915-8929, 2019.](#)

405 Twomey, S., 1977: The Influence of Pollution on the Shortwave Albedo of Clouds. *J. Atmos. Sci.*,  
406 34, 1149–1152, <https://doi.org/10.1175/1520-0469>, 1977.

407 Yarwood, G., S. Rao, M. Yocke, and G.Z. Whitten, Updates to the Carbon Bond Mechanism:  
408 CB05. US EPA Final Report, 161 pp., 2005. [Available at  
409 [http://www.camx.com/publ/pdfs/CB05\\_Final\\_Report\\_120805.pdf](http://www.camx.com/publ/pdfs/CB05_Final_Report_120805.pdf)]

410 Yu, F. and Luo, G.: Simulation of particle size distribution with a global aerosol model:  
411 contribution of nucleation to aerosol and CCN number concentrations, *Atmos. Chem. Phys.*,  
412 9, 7691-7710, <https://doi.org/10.5194/acp-9-7691-2009>, 2009.

413 Yu, F., A secondary organic aerosol formation model considering successive oxidation aging and  
414 kinetic condensation of organic compounds: global scale implications, *Atmos. Chem. Phys.*,  
415 11, 1083-1099, doi:10.5194/acp-11-1083-2011, 2011.

416 Yu, F., G. Luo, and X. Ma, Regional and global modelling of aerosol optical properties with a size,  
417 composition, and mixing state resolved particle microphysics model, *Atmos. Chem. Phys.*, 12,  
418 5719-5736, doi:10.5194/acp-12-5719-2012, 2012.

419 Yu, F., Luo, G., Pryor, S. C., Pillai, P. R., Lee, S. H., Ortega, J., Schwab, J. J., Hallar, A. G.,  
420 Leaitch, W. R., Aneja, V. P., Smith, J. N., Walker, J. T., Hogrefe, O., and Demerjian, K. L.:  
421 Spring and summer contrast in new particle formation over nine forest areas in North America,  
422 *Atmos. Chem. Phys.*, 15, 13993-14003, doi:10.5194/acp-15-13993-2015, 2015.

423 [Yu, F., Luo, G., Nadykto, A. B., and Herb, J.: Impact of temperature dependence on the possible](#)  
424 [contribution of organics to new particle formation in the atmosphere, \*Atmos. Chem. Phys.\*, 17,](#)  
425 [4997-5005, <https://doi.org/10.5194/acp-17-4997-2017>, 2017.](#)

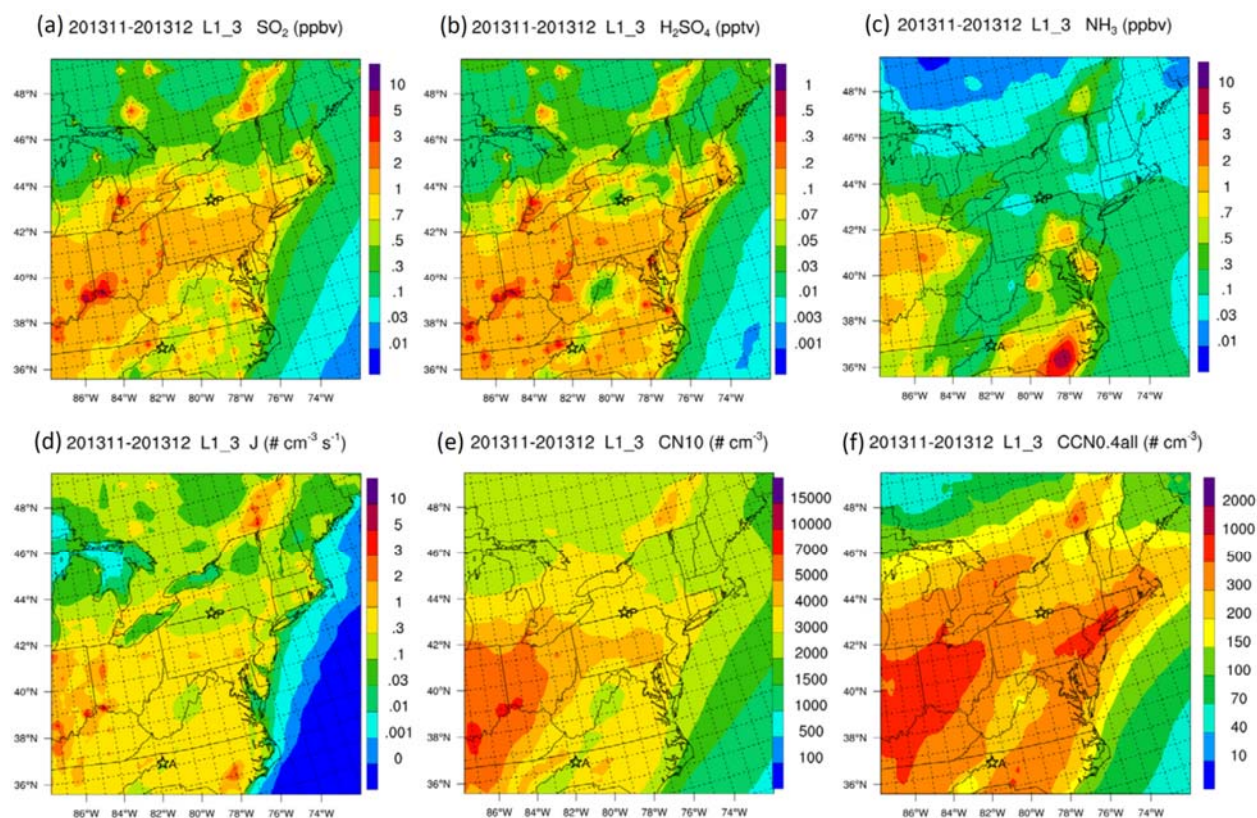
426 Yu, F., Nadykto, A. B., Herb, J., Luo, G., Nazarenko, K. M., and Uvarova, L. A.: H<sub>2</sub>SO<sub>4</sub>-H<sub>2</sub>O-

427 NH<sub>3</sub> ternary ion-mediated nucleation (TIMN): Kinetic-based model and comparison with  
428 CLOUD measurements, *Atmos. Chem. Phys.*,18, 17451-17474, [https://doi.org/10.5194/acp-](https://doi.org/10.5194/acp-18-17451-2018)  
429 18-17451-2018, 2018.

430 [Yu, H., A. G. Haller, Y. You, A. Sedlacek, S. Springston, V. P. Kanawade, Y.-N. Lee, J. Wang, C. Kuang,](#)  
431 [R. L. McGraw, I. McCubbin, J. Mikkala, and S.-H. Lee, Sub-3 nm particles observed at the](#)  
432 [coastal and continental sites in the United States, \*J. Geophys. Res.\* \*\*119\*\*,](#)  
433 [Doi:10.1029/2013JD020841, 2014.](#)

434

435

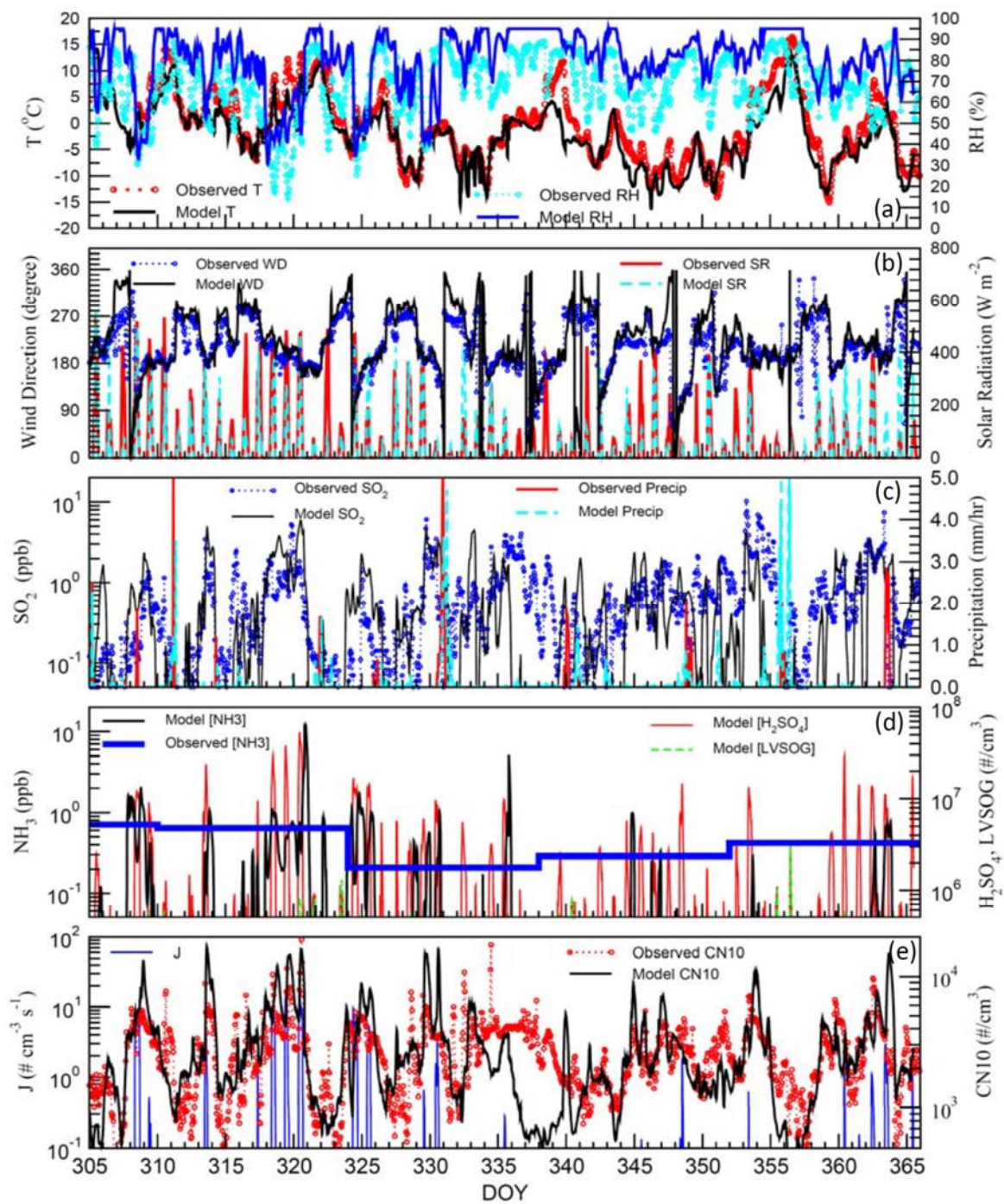


436

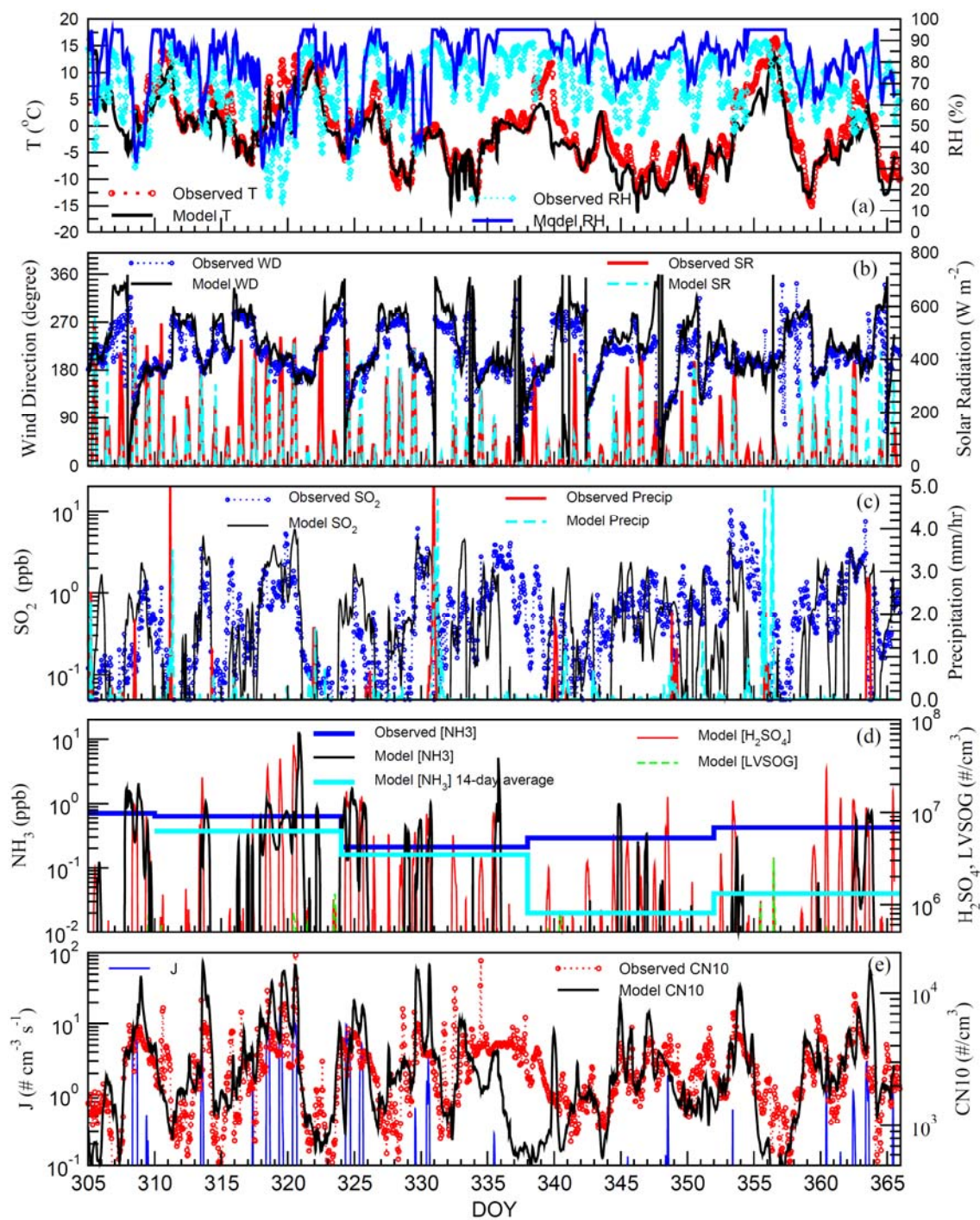
437 **Figure 1.** Horizontal spatial distribution of WRF-Chem-APM simulated average wintertime (2013  
438 November–December) (a) [SO<sub>2</sub>], (b) [H<sub>2</sub>SO<sub>4</sub>], (c) [NH<sub>3</sub>], (d) nucleation rate (*J*), (e) number  
439 concentration of condensation nuclei > 10 nm (CN10), and (f) cloud condensation nuclei at  
440 supersaturation 0.4% (CCN0.4) in the lower boundary layer (~ 0 – 400 m above surface, first three  
441 model layers) over the Northeastern United States (NEUS). Measurement sites Appalachian State

442 University (APP), North Carolina (A) and Pinnacle State Park (P), New York are marked on the  
443 maps.

444

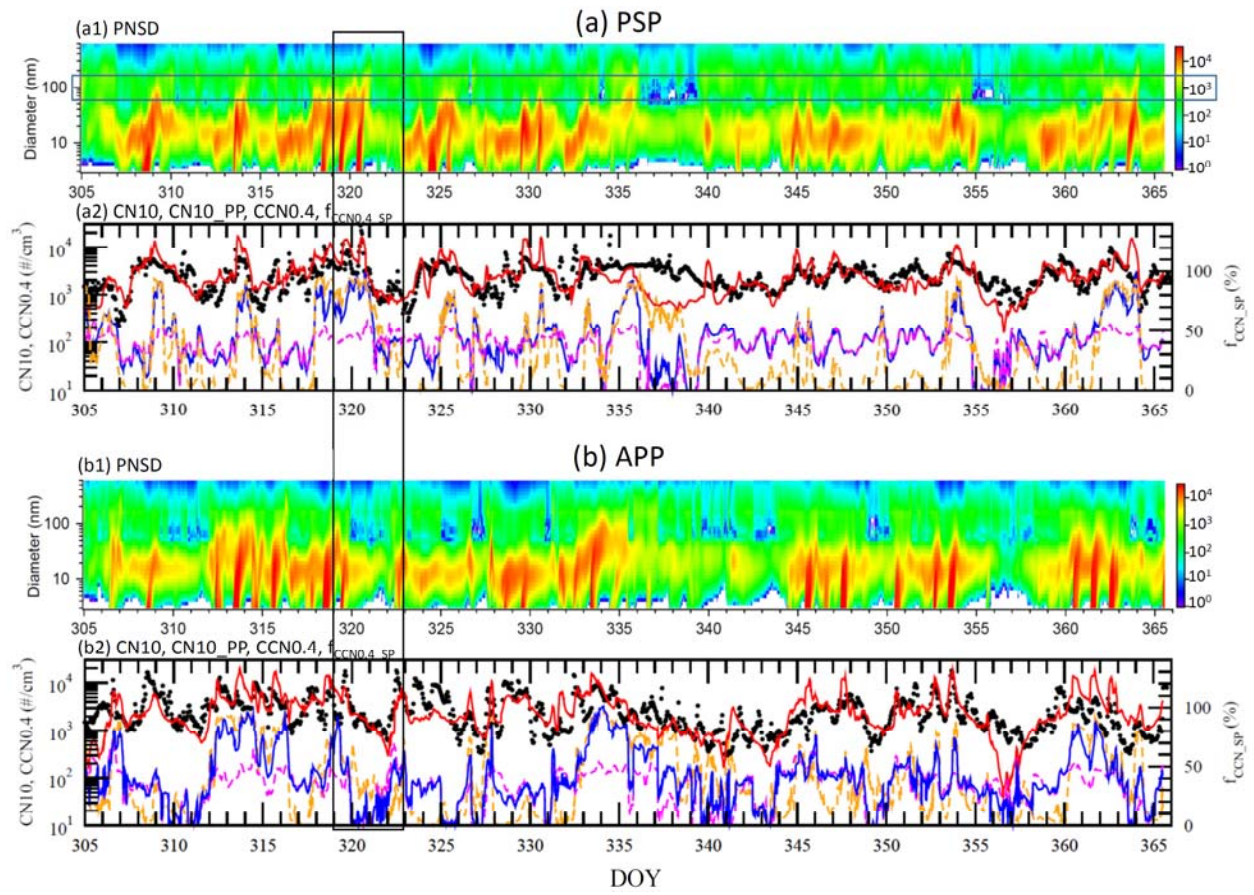


445



446

447 **Figure 2.** Modeled diurnal variability of wintertime (November–December 2013) (a) temperature  
 448 (T) and relative humidity (RH), (b) wind direction (WD) and solar radiation (SR), (c) [SO<sub>2</sub>] and  
 449 precipitation, (d) [NH<sub>3</sub>], [H<sub>2</sub>SO<sub>4</sub>], and concentration of low-volatile secondary organic gas ([LV-  
 450 SOG]), and (e) nucleation rate (*J*) and CN10 at the Pinnacle State Park (PSP) site compared with  
 451 in situ measurements. X-axis is the day of year (DOY).



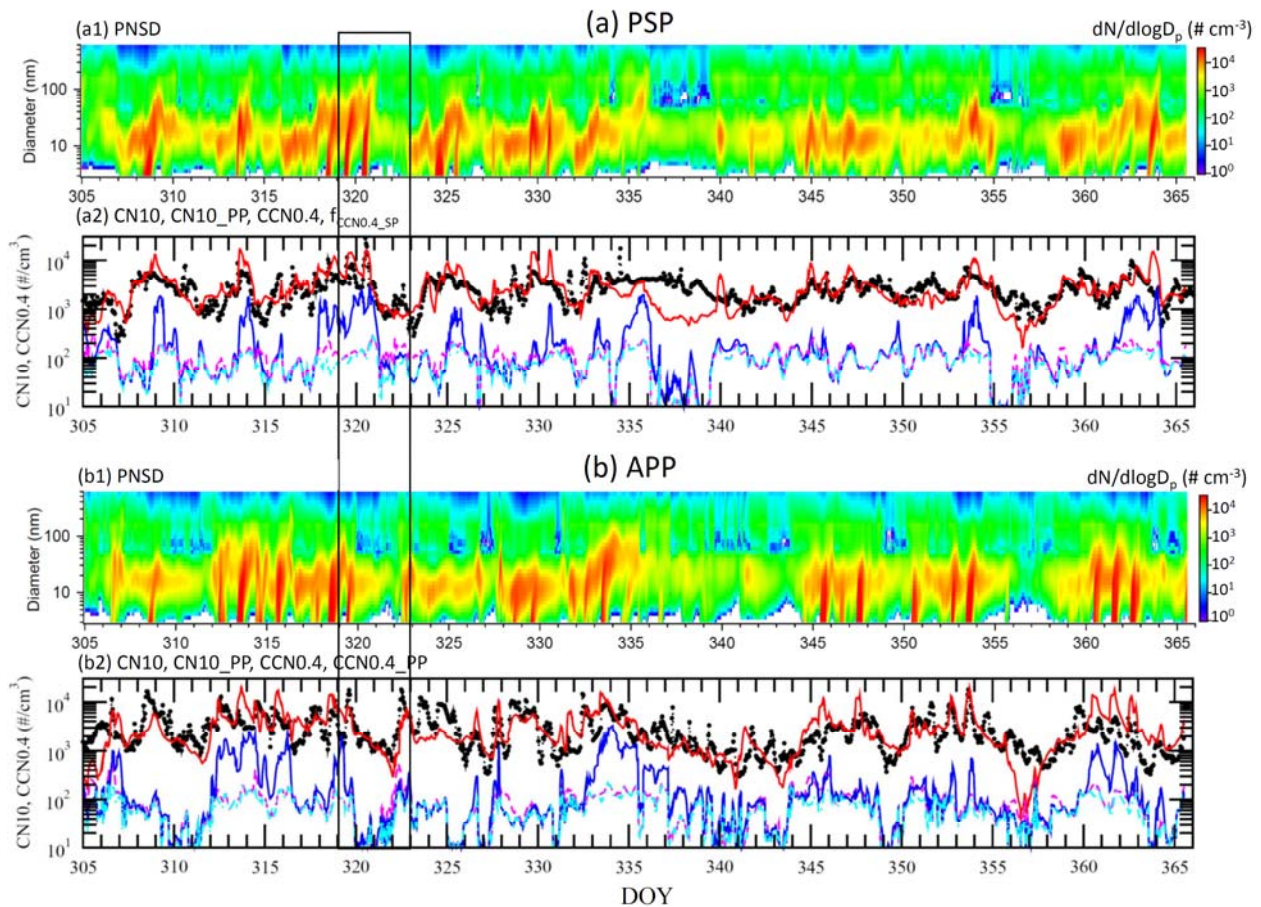


**Figure 3.** For the (a) PSP and (b) APP sites in the NEUS: Modeled wintertime (November–December 2013) evolution of particle number size distributions (PNSD, a1, b1), and time series (a2, b2) of CN10 (red line), CN10 due to primary particles (CN10\_PP, dashed magenta line), CCN0.4 (blue line), and percentage of CCN0.4 associated with secondary due to primary particles ( $f_{\text{CCN\_SP\_CCN0.4\_PP}}$ , dashed orange-cyan line). In a2 and b2, CN10 values from observations (black circles) are also shown for comparison. The model results are for the model surface layer (~0–100 m above surface). Selected 4-day period from November 15–18, 2013 with nucleation events and non-events is marked within a black rectangle.

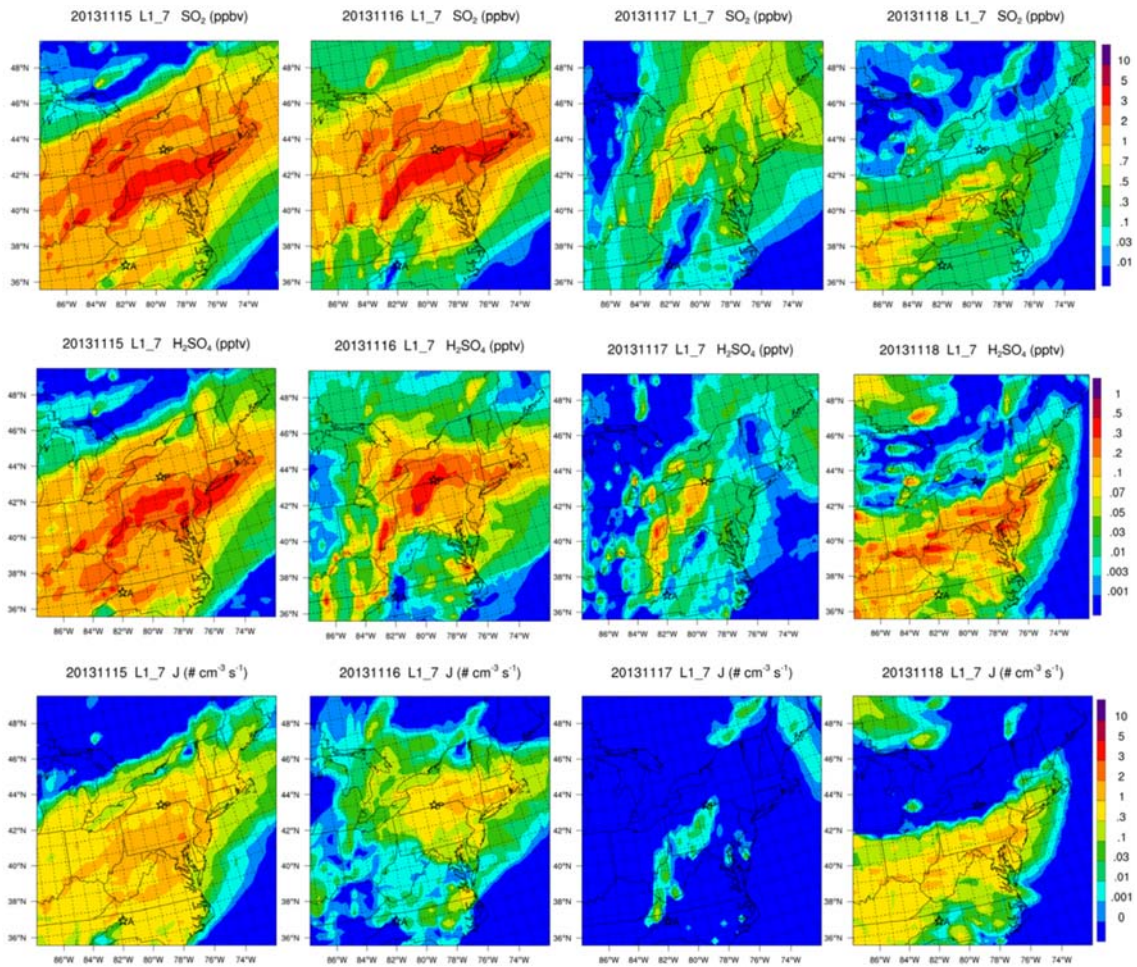


**Figure 4.** For the each of the 4-day period from (left to right) November 15–18, 2013: (top to bottom) modeled horizontal spatial distribution of [SO<sub>2</sub>], [H<sub>2</sub>SO<sub>4</sub>], and nucleation rate (*J*) over the NEUS, with the measurement sites Pinnacle State Park (P) and APP (A) marked on the maps.

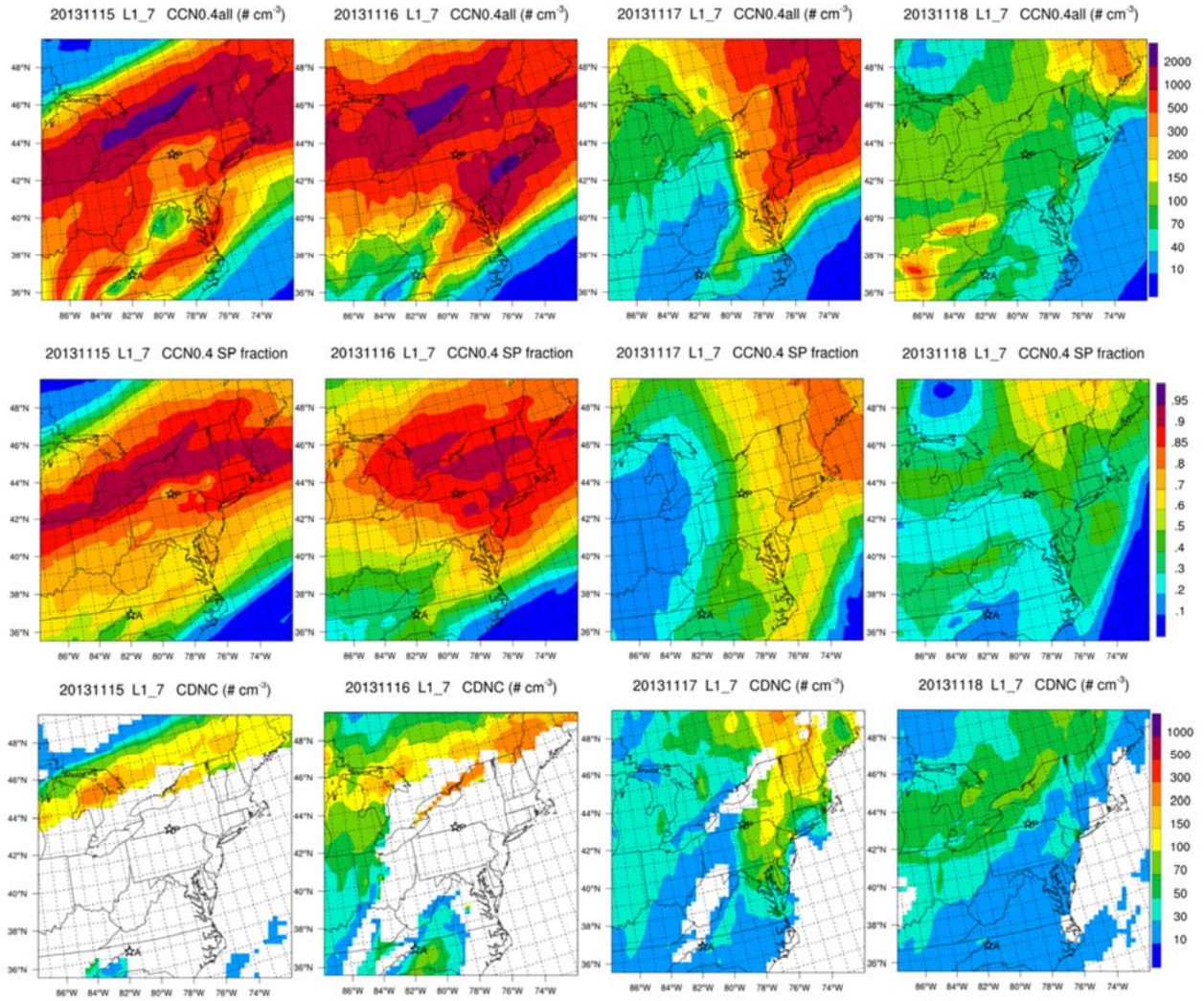


**Figure 5.** For the each of the 4-day period from (left to right) November 15–18, 2013: (top) CCN0.4 and (middle) its secondary particle fraction (CCN0.4 SP), and (bottom) cloud droplet (CDNC) modeled horizontal spatial distribution over the NEUS, with the measurement sites Pinnacle State Park (P) and APP (A) marked on the maps.

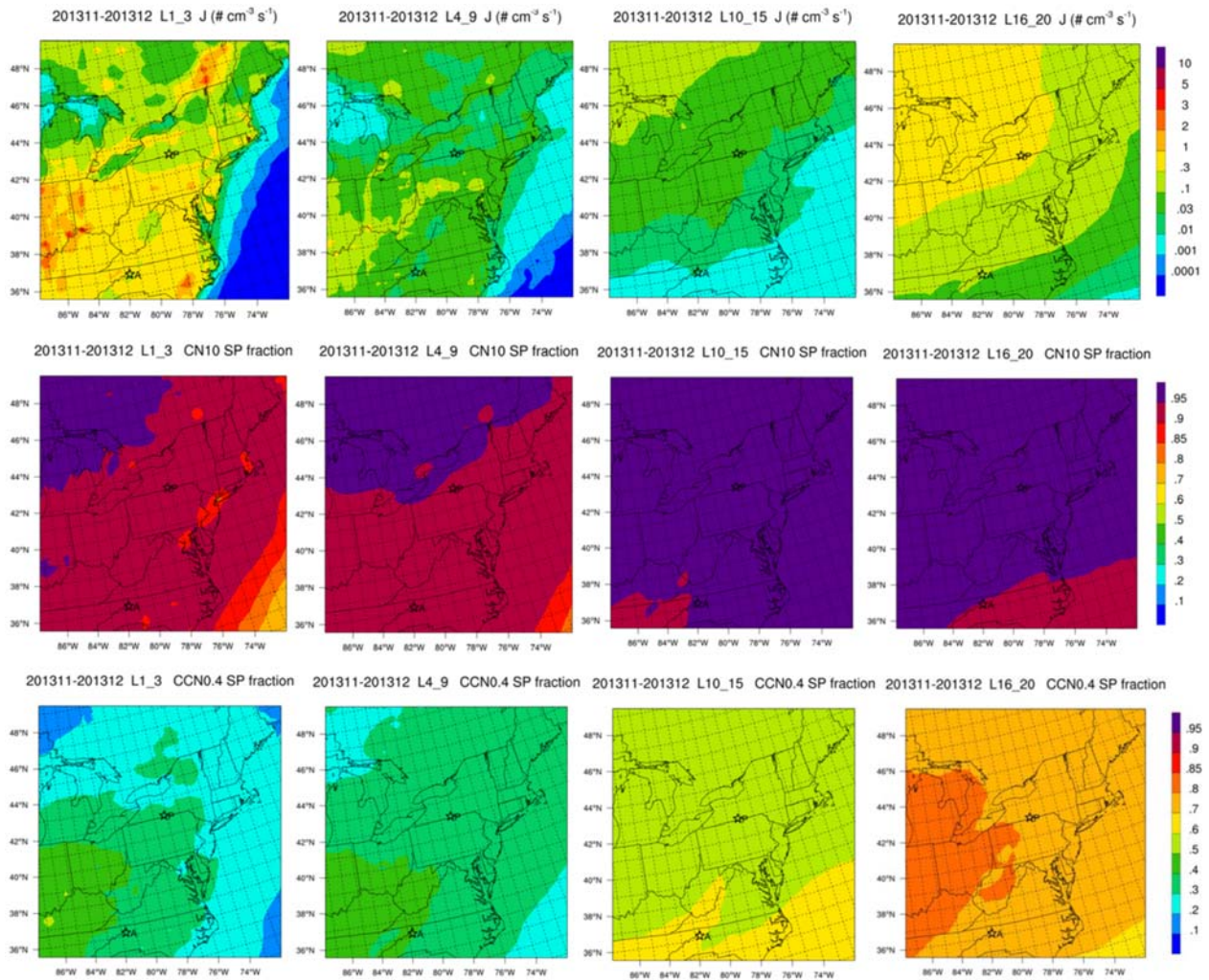


**Figure 6.** Modeled average wintertime (2013 November–December) (top) nucleation rate ( $J$ ), (bottom) CN SP fraction, and (bottom) CCN0.4 SP fraction for (left to right) the surface layer, lower, middle, and upper troposphere.